

The public reporting burden for this collection of information is estimated to average 1 hour per response, including the time for reviewing instructions, searching existing data sources, gathering and maintaining the data needed, and completing and reviewing the collection of information. Send comments regarding this burden estimate or any other aspect of this collection of information, including suggestions for reducing this burden, to Washington Headquarters Services, Directorate for Information Operations and Reports, 1215 Jefferson Davis Highway, Suite 1204, Arlington VA, 22202-4302. Respondents should be aware that notwithstanding any other provision of law, no person shall be subject to any penalty for failing to comply with a collection of information if it does not display a currently valid OMB control number.
PLEASE DO NOT RETURN YOUR FORM TO THE ABOVE ADDRESS.

1. REPORT DATE (DD-MM-YYYY) 18-06-2018	2. REPORT TYPE Final Report	3. DATES COVERED (From - To) 26-Jan-2015 - 1-Apr-2018
---	--------------------------------	--

4. TITLE AND SUBTITLE Final Report: The Potential of Using Microwave Emission in Detecting Freeze and Thaw States	5a. CONTRACT NUMBER W911NF-15-1-0070
	5b. GRANT NUMBER
	5c. PROGRAM ELEMENT NUMBER 611104

6. AUTHORS	5d. PROJECT NUMBER
	5e. TASK NUMBER
	5f. WORK UNIT NUMBER

7. PERFORMING ORGANIZATION NAMES AND ADDRESSES CUNY - New York City College of Technol 300 Jay Street Brooklyn, NY 11201 -1909	8. PERFORMING ORGANIZATION REPORT NUMBER
---	--

9. SPONSORING/MONITORING AGENCY NAME(S) AND ADDRESS (ES) U.S. Army Research Office P.O. Box 12211 Research Triangle Park, NC 27709-2211	10. SPONSOR/MONITOR'S ACRONYM(S) ARO
	11. SPONSOR/MONITOR'S REPORT NUMBER(S) 66551-EV.12

12. DISTRIBUTION AVAILABILITY STATEMENT
Approved for public release; distribution is unlimited.

13. SUPPLEMENTARY NOTES
The views, opinions and/or findings contained in this report are those of the author(s) and should not be construed as an official Department of the Army position, policy or decision, unless so designated by other documentation.

14. ABSTRACT

15. SUBJECT TERMS

16. SECURITY CLASSIFICATION OF:			17. LIMITATION OF ABSTRACT	15. NUMBER OF PAGES	19a. NAME OF RESPONSIBLE PERSON Hamidreza Norouzi
a. REPORT UU	b. ABSTRACT UU	c. THIS PAGE UU	UU		19b. TELEPHONE NUMBER 718-260-5410

RPPR Final Report
as of 04-Sep-2018

Agency Code:

Proposal Number: 66551EV

Agreement Number: W911NF-15-1-0070

INVESTIGATOR(S):

Name: Hamidreza Norouzi
Email: hnorouzi@citytech.cuny.edu
Phone Number: 7182605410
Principal: Y

Organization: **CUNY - New York City College of Technology**

Address: 300 Jay Street, Brooklyn, NY 112011909

Country: USA

DUNS Number: 611930657

EIN: 363328437

Report Date: 01-Jul-2018

Date Received: 18-Jun-2018

Final Report for Period Beginning 26-Jan-2015 and Ending 01-Apr-2018

Title: The Potential of Using Microwave Emission in Detecting Freeze and Thaw States

Begin Performance Period: 26-Jan-2015

End Performance Period: 01-Apr-2018

Report Term: 0-Other

Submitted By: Hamidreza Norouzi

Email: hnorouzi@citytech.cuny.edu

Phone: (718) 260-5410

Distribution Statement: 1-Approved for public release; distribution is unlimited.

STEM Degrees: 1

STEM Participants: 3

Major Goals: In this project, the potential of using passive microwave (PMW) emissivity instead of the direct use of Tb information in the detection and analysis of FT states will be investigated. The advantage of using emissivity instead of Tb is that emissivity values are expected to provide invaluable information about the state of the surface since the dielectric constant of the surface changes significantly during the FT process. However, the direct use of Tb is typically fraught with atmospheric and temperature noises. Transition between freeze and thaw states depends on the amount of heat energy the surface receives or releases and on the corresponding change in seasonal and diurnal temperature. This project aims to develop a method using emissivity estimates from two similar kind of passive microwave sensors (AMSR-E and AMSR2) for FT states detection.

Main Objectives:

- Instantaneous Emissivity Retrieval from AMSR-E and AMSR2
(Completed 100%)
- Algorithm for Freeze and Thaw states Detection
(Completed 100%)

Accomplishments: See attached report.

Training Opportunities: One PhD student (Zahra Sharif) and one masters student (Abdou BAH) were involved in this research. Students became familiar with the remote sensing applications especially diurnal variation of surface temperature.

RPPR Final Report as of 04-Sep-2018

Results Dissemination: 1. Prakash, S., H. Norouzi, M. Azarderakhsh, R. Blake, C. Prigent, and R. Khanbilvardi, 2018: "Estimation of consistent global microwave land surface emissivity from AMSR-E and AMSR2 observations", *Journal of Applied Meteorology and Climatology*, 10.1175/JAMC-D-17-0213.1, 2018.
2. Shati, F., S. Prakash, H. Norouzi, and R. Blake: "Assessment of differences between near-surface air and soil temperatures for reliable detection of high-latitude freeze and thaw states", *Cold Regions Science and Technology*, doi:10.1016/j.coldregions.2017.10.007, 2018.
3. Prakash, S., H. Norouzi, M. Azarderakhsh, R. Blake, and R. Khanbilvardi, 2017: Potential of satellite-based land emissivity estimates for the detection of high-latitude freeze and thaw states, *Geophysical Research Letters*, 44(5), 2336-2342, doi:10.1002/2017GL072560.
4. Prakash, S., H. Norouzi, M. Azarderakhsh, and R. Blake, 2017: Fine temporal resolution freeze and thaw states using combination of microwave land surface emissivity estimates, "IEEE International Geoscience and Remote Sensing Symposium", 23-28 Jul, Fort Worth, Texas, USA.
5. Prakash, S., H. Norouzi, M. Azarderakhsh, R. Blake, and R. Khanbilvardi, 2017: Detection of freeze and thaw states from satellite passive microwave global land emissivity estimates, "2017 NOAA Satellite Conference", 17-20 Jul, New York, USA.
6. Prakash, S., H. Norouzi, M. Azarderakhsh, R. Blake, and F. Shati, 2016: A novel approach for freeze/thaw detection using satellite-based land emissivity estimates, "AGU Fall Meeting 2016", 12-16 Dec, San Francisco, USA.
7. Prakash, S., Norouzi, H., Azarderakhsh, M., Blake, R., and Tesfagiorgis K.: "Global Land Surface Emissivity Estimation From AMSR2 Observations", *IEEE Geoscience and Remote Sensing Letters*, DOI: 10.1109/LGRS.2016.2581140, 2016.
8. Shati, F., S., Prakash, H., Norouzi, Evaluation of Differences among Near-surface Air Temperature, Land Surface Temperature and Soil Temperature Using Remote Sensing and Ground-Based Observations, American Meteorological Society (AMS) annual meeting, Washington, January 2017.
9. Prakash, S., H. Norouzi, M. Azarderakhsh, R. Blake, and F. Shati, 2017: Daily Freeze/Thaw Detection from Passive Microwave Global Land Surface Emissivity", "AGU Fall Meeting 2017", Dec 2017, New Orleans, LA, USA.

Honors and Awards: Nothing to Report

Protocol Activity Status:

Technology Transfer: Nothing to Report

PARTICIPANTS:

Participant Type: PD/PI

Participant: Hamid Norouzi

Person Months Worked: 4.00

Project Contribution:

International Collaboration:

International Travel:

National Academy Member: N

Other Collaborators:

Funding Support:

Participant Type: Co-Investigator

Participant: Reginald Blake

Person Months Worked: 3.00

Project Contribution:

International Collaboration:

International Travel:

National Academy Member: N

Other Collaborators:

Funding Support:

Participant Type: Postdoctoral (scholar, fellow or other postdoctoral position)

Participant: Satya Prakash

Person Months Worked: 6.00

Funding Support:

RPPR Final Report
as of 04-Sep-2018

Project Contribution:
International Collaboration:
International Travel:
National Academy Member: N
Other Collaborators:

Participant Type: Postdoctoral (scholar, fellow or other postdoctoral position)

Participant: Christopher Beale

Person Months Worked: 15.00

Funding Support:

Project Contribution:
International Collaboration:
International Travel:
National Academy Member: N
Other Collaborators:

Participant Type: Graduate Student (research assistant)

Participant: Zahra Sharif

Person Months Worked: 10.00

Funding Support:

Project Contribution:
International Collaboration:
International Travel:
National Academy Member: N
Other Collaborators:

Participant Type: Research Experience for Undergraduates (REU) Participant

Participant: Farjana Shati

Person Months Worked: 6.00

Funding Support:

Project Contribution:
International Collaboration:
International Travel:
National Academy Member: N
Other Collaborators:

Participant Type: Graduate Student (research assistant)

Participant: Abdou BAH

Person Months Worked: 2.00

Funding Support:

Project Contribution:
International Collaboration:
International Travel:
National Academy Member: N
Other Collaborators:

ARTICLES:

RPPR Final Report
as of 04-Sep-2018

Publication Type: Conference Paper or Presentation **Publication Status:** 1-Published
Conference Name: American Geophysical Union (AGU) Fall Meeting 2015
Date Received: 30-Aug-2016 Conference Date: 15-Dec-2015 Date Published: 19-Dec-2015
Conference Location: San Francisco, CA
Paper Title: The Feasibility Study of Using Microwave Emissivity in Detecting Freeze and Thaw States
Authors: Hamidreza Norouzi, Satya Prakash, Marzi Azarderakhsh, Reginald Blake
Acknowledged Federal Support: **Y**

Publication Type: Conference Paper or Presentation **Publication Status:** 1-Published
Conference Name: IEEE Geoscience and Remote Sensing Society, the International Geoscience and Remote Sensing Symposium 2016 (IGARSS)
Date Received: 30-Aug-2016 Conference Date: 10-Jul-2016 Date Published: 15-Jul-2016
Conference Location: Beijing, China
Paper Title: HIGH-LATITUDE FREEZE AND THAW STATES DETECTION USING SATELLITE-BASED MICROWAVE LAND SURFACE EMISSIVITY ESTIMATES
Authors: Hamidreza Norouzi, Satya Prakash, Marzi Azarderakhsh, Reginald Blake, Christian Campo
Acknowledged Federal Support: **Y**

Publication Type: Conference Paper or Presentation **Publication Status:** 1-Published
Conference Name: IEEE International Geoscience and Remote Sensing Symposium
Date Received: 18-Jun-2018 Conference Date: 24-Jul-2017 Date Published:
Conference Location: Fort Worth TX
Paper Title: Fine temporal resolution freeze and thaw states using combination of microwave land surface emissivity estimates
Authors: Satya Prakash, Hamid Norouzi, Marzieh Azarderakhsh, and Reginald Blake
Acknowledged Federal Support: **Y**

Publication Type: Conference Paper or Presentation **Publication Status:** 1-Published
Conference Name: AGU Fall Meeting 2017
Date Received: 18-Jun-2018 Conference Date: 12-Dec-2017 Date Published: 12-Dec-2017
Conference Location: New Orleans, LA
Paper Title: Daily Freeze/Thaw Detection from Passive Microwave Global Land Surface Emissivity Data
Authors: Satya Prakash, Hamid Norouzi, Marzi Azarderakhsh, Reginald Blake, Reza Khanbilvardi
Acknowledged Federal Support: **Y**

Publication Type: Conference Paper or Presentation **Publication Status:** 1-Published
Conference Name: AGU Fall Meeting 2016
Date Received: 18-Jun-2018 Conference Date: 16-Dec-2016 Date Published: 16-Dec-2016
Conference Location: San Francisco, CA
Paper Title: Assessment of Differences Among Air Temperature, Land Surface Temperature and Soil Temperature Using Remote Sensing and Ground-Based Observations
Authors: Farjana Shati, Satya Prakash, Hamid Norouzi, Reginald Blake
Acknowledged Federal Support: **Y**

Publication Type: Conference Paper or Presentation **Publication Status:** 1-Published
Conference Name: AGU Fall Meeting 2016
Date Received: 18-Jun-2018 Conference Date: 16-Dec-2016 Date Published: 16-Dec-2016
Conference Location: San Francisco, CA
Paper Title: A Novel Approach For Freeze/Thaw Detection Using Satellite-Based Land Emissivity Estimates
Authors: Satya Prakash, Hamid Norouzi, Marzi Azarderakhsh, Reginald Blake, Reza Khanbilvardi
Acknowledged Federal Support: **Y**

RPPR Final Report
as of 04-Sep-2018

Publication Type: Conference Paper or Presentation

Publication Status: 3-Accepted

Conference Name: IEEE International Geoscience and Remote Sensing Symposium

Date Received: 18-Jun-2018

Conference Date: 24-Jul-2018

Date Published:

Conference Location: Valencia, Spain

Paper Title: THE HIGH TEMPORAL DETECTION OF LAND SURFACE FREEZE AND THAW STATES VIA A COMBINATION OF PASSIVE MICROWAVE ESTIMATES

Authors: Hamid Norouzi, Satya Prakash, Marzi Azarderakhsh, Christopher Beale, Reginald Blake

Acknowledged Federal Support: **Y**

The Potential of Using Microwave Emission in Detecting Freeze and Thaw States

(Jan, 26 2015 to Apr, 01 2018)

PI: Hamid Norouzi

Co-I: Reginlad Blake

New York City College of Technology, The City University of New York

1. Introduction

Ground freezing in high-latitude areas either through seasonally freezing or by the development of permafrost usually involves subsurface processes, which can affect hydrology, biochemistry, health, and human activities. However, seasonal freezing and thawing is controlled by temperature, soil texture, soil moisture content, vegetation, and microclimate. On an average, more than one-third of the global land area undergoes seasonal freezing and thawing process. Freeze and thaw (FT) process has a profound impact on the terrestrial water cycle, net primary productivity, carbon cycle, surface energy budget and hence the global climate system. A major portion of the Northern Hemisphere, especially high-latitude regions, is subject to seasonal freezing and thawing process. Since ground-observations of FT states in boreal regions are generally sparse and inconsistent, the monitoring of FT process in these areas is difficult. On the other hand, remote sensing applications in the active and passive microwave have shown to be reliable in monitoring dynamics at regional and global scales.

Microwave remote sensing provides more frequent observations (at least twice a day and more frequent in the Polar regions) and is less affected by clouds. The dielectric changes between freeze and thaw states make the microwave remote sensing unique for characterizing the surface FT process. Passive microwave (PMW) sensors benefit from rather more spatial coverage, and they are fixed by frequency, incidence angle, and polarization. The change in dielectric can dramatically affect the brightness temperature (T_b) signal when water transits from the liquid to the solid phase. Therefore, PMW studies have been used to investigate thresholds to detect FT states and a global daily FT product has been developed. However, the problem with directly using T_bs from PMW sensors is that they are affected by water vapor in the atmosphere even if cloud-free measurements are utilized. This problem is more highlighted in higher frequencies (above 19 GHz). Furthermore, T_bs depend on both the temperature and the emissivity values of the footprint. Emissivity can be representative of the surface state and change in dielectric. However, the presence of physical temperature can interfere with the analysis of the signal when T_bs are used in FT states detection.

In this project, the potential of using PMW emissivity instead of the direct use of T_b information in the detection and analysis of FT states was investigated. The advantage of using emissivity instead of T_b is that emissivity values are expected to provide invaluable information about the state of the surface since the dielectric constant of the surface changes significantly during the FT process. However, the direct use of T_b is typically fraught with atmospheric and temperature noises. Transition between freeze and thaw states depends on the amount of heat energy the surface receives or releases and on the corresponding change in seasonal and diurnal temperature. This project aims to develop a method using emissivity estimates from two similar kind of passive microwave sensors (AMSR-E and AMSR2) for FT states detection.

2. Global Microwave Land Surface Emissivity Estimation from AMSR-E and AMSR2

Accurate estimation of passive microwave land surface emissivity (LSE) is crucial for numerical weather prediction model data assimilation, for microwave retrievals of land precipitation and atmospheric profiles, and for better understanding of land surface and sub-surface characteristics. Global instantaneous LSE was estimated for the 9-year period of October 2002 to September 2011 from the Advanced Microwave Scanning Radiometer - Earth Observing System (AMSR-E) and for the 5-year period of July 2012 to June 2017 from the Advanced Microwave Scanning Radiometer – 2 (AMSR2) sensors. Estimates of LSE from both sensors were obtained by using an updated algorithm that minimizes the discrepancy between the differences in penetration depths from microwave and infrared remote sensing observations. Concurrent ancillary datasets such as skin temperature from the Moderate Resolution Imaging Spectroradiometer (MODIS) and profiles of air temperature and humidity from the Atmospheric Infrared Sounder (AIRS) were used for the computation of more reliable LSE estimates from AMSR-E and AMSR2 sensors. The latest collection 6 of MODIS skin temperature was used for the LSE estimation, and the differences between collections 6 and 5 are also comprehensively assessed.

2.1 AMSR-E and AMSR2 data

The Aqua and the Global Change Observation Mission 1st – Water (GCOM-W1) satellites are the members of the “Afternoon Constellation” or “A-Train”, whose equatorial crossing times are about 1:30 p.m./a.m. The Aqua satellite was launched on May 04, 2002 by the National Aeronautics and Space Administration (NASA), and among the sensors it carries the AMSR-E, the Atmospheric Infrared Sounder (AIRS), and the Moderate Resolution Imaging Spectroradiometer (MODIS). The overall goal of the Aqua satellite and its suite of sensors is to study water in the Earth-atmosphere-biosphere system. However, AMSR-E stopped producing data in October, 2011. On May 18, 2012, the Japan Aerospace Exploration Service (JAXA) launched the GCOM-W1 satellite. The satellite had the AMSR2 instrument onboard with the aim of studying changes in water circulation. AMSR-E was a six-frequency dual-polarized PMW radiometer that measured Tbs at 6.925, 10.65, 18.7, 23.8, 36.5, and 89.0 GHz (Kawanishi et al., 2003). AMSR2 has sensor characteristics similar to those of its predecessor AMSR-E, but it also included improvements such as an additional 7.3 GHz channel for radiofrequency interference mitigation and also improved calibration (Okuyama and Imaoka, 2015). Like AMSR-E, AMSR2 has a conical scan mechanism and it obtains data over a ~1450 km swath with 55° incidence angle. In this study, level-3 global swath spatially resampled Tbs at 0.25° spatial resolution for all the frequency channels of AMSR-E (version 7) for October 2002 to September 2011 and AMSR2 (version 2.2) for July 2012 to June 2017 were used. These datasets were obtained from the GCOM-W research product distribution service at the JAXA.

2.2 Ancillary satellite data

To mitigate the atmospheric effects from the PMW measurements of Tbs, near-simultaneous infrared-based LST, and profiles of air temperature and humidity were used. The latest collection of the MODIS version 6 (V6) cloud-free land surface temperature daily L3 swath global product (e.g., MYD11C1; Wan, 2014) available at 0.05° climate modeling grid (~5.6 km at the equator) were used. Large-scale changes in V6 of the global LST product as compared to its predecessor V5 were also assessed. The daily level-3 globally gridded integrated water vapor and air temperature profiles from the AIRS infrared-only V6 (e.g., AIRS3STD; Susskind et al., 2014) available at 1° spatial resolutions were used. It is to be noted that version 6 of ancillary data from both MODIS and AIRS sensors, mounted on the sun-synchronous

Aqua satellite, under clear-sky conditions were used. Thus, the estimated LSE would effectively benefit from the concurrence of satellite observations.

In order to compare mean features of the estimated LSE, updated version of Tool to Estimate Land-Surface Emissivities at Microwave frequencies (e.g., TELSEM2) climatology was used. TELSEM2 was developed to provide a reliable parameterization of LSE for frequencies up to 700 GHz for advancing data assimilation of radiances in the numerical weather prediction models (Wang et al., 2017). The emissivity parameterization between 19 and 85 GHz is anchored to a monthly mean climatology of LSE computed from the SSM/I observations between 1993 and 2000 at 0.25° equal-area grid.

2.3 Method for LSE estimation

Since the spatial resolutions of PMW-based Tbs and infrared-based ancillary data are different, all these orbital data were re-projected to a common equal-area grid (0.25° at equator). The instantaneous global cloud-free land surface emissivity (ϵ) from AMSR-E and AMSR2 Tbs at polarization (p) and frequency (v) condition is computed using the following expression (Prigent et al., 2006):

$$\epsilon_{(p,v)} = \frac{Tb_{(p,v)} - T\uparrow - T\downarrow e^{-\tau(0,H)/\mu}}{e^{-\tau(0,H)/\mu}(T_s - T\downarrow)} \quad (1)$$

where, $T\uparrow$ and $T\downarrow$ are upward and downward contribution of Tbs from the atmosphere at the surface, respectively and they depend on incidence angle, atmospheric absorption and extinction. The atmospheric temperature and humidity play key role in the determination of these parameters through a suitable microwave radiative transfer model (Norouzi et al., 2011). T_s stands for skin temperature or LST, μ be the cosine of incidence angle, and τ denotes the atmospheric opacity between two altitudes. The estimated cloud-free land emissivity using equation (1) may produce inconsistent LSE values between day and night up to 12% due to the use of infrared-based LST instead of effective temperature at the depth of PMW observations. There exists a considerable difference in the diurnal cycle amplitude and phase between PMW-based Tbs and infrared-based LST, primarily in arid regions where moisture and vegetation are scarce and they cover about 45% of the global land areas (Norouzi et al., 2012, 2015b). To minimize this difference and produce more accurate LSE estimates, a statistical correction factor is applied to the MODIS LST over arid regions. The correction factor for the MODIS LST is computed for each month based on the mean passive microwave Tbs for day and night overpasses based on the following equation:

$$T_{s(t)}^C = T_{s(t)} \pm \frac{\overline{Tb_{day(t)}} - \overline{Tb_{night(t)}}}{2} \quad (2)$$

where, $\overline{Tb_{day(t)}}$ and $\overline{Tb_{night(t)}}$ are the mean composite Tbs for all the day and night overpasses for a specific month, $T_{s(t)}^C$ is the corrected effective temperature consistent with PMW data, and $T_{s(t)}$ is the mean daily skin temperature. A detailed description of this statistical method is provided by Prakash et al. (2016). However, this statistical method is suitable for the estimation of instantaneous cloud-free LSE. Hence, the LSE estimates presented in this study use an improved algorithm and common observational input datasets. The errors in LSE retrieval due to the uncertainties in ancillary atmospheric datasets were explicitly quantified by Norouzi et al. (2011). Thus, the use of concurrent ancillary datasets would essentially reduce the uncertainty in the LSE estimates.

Figure 1 shows the spatial distributions of mean daytime (ascending orbits) and nighttime (descending orbits) LST from V6 and V5 products and their corresponding differences for the period of

2003 to 2015. The broad-scale mean features such as higher LST over the arid regions and lower LST over the polar regions, and cooler LST in nighttime than daytime associated with surface insolation due to the solar zenith angle are similar in both the versions. Larger differences in daytime and nighttime LST can be seen over the arid regions of Africa and Australia. However, a notable difference in magnitude between V6 and V5 can be seen primarily over the arid regions. V5 shows 2-4°C less LST than V6 during the daytime over the Saudi Arabia, Africa, and South America. However, such underestimation of LST by V5 is mainly concentrated over the desert areas (Sahara Desert, Arabian Desert, and Gobi Desert) in the descending overpasses. Arid regions are the places where LSE uncertainty is high and hence accurate LST is crucial over these regions. Moreover, a noticeable overestimation of nighttime LST by V5 as compared to V6 can be observed over the eastern part of the Southern Polar regions. The underestimation of LST in V5 over the arid regions was found to be more than 2K as compared to ground-based observations.

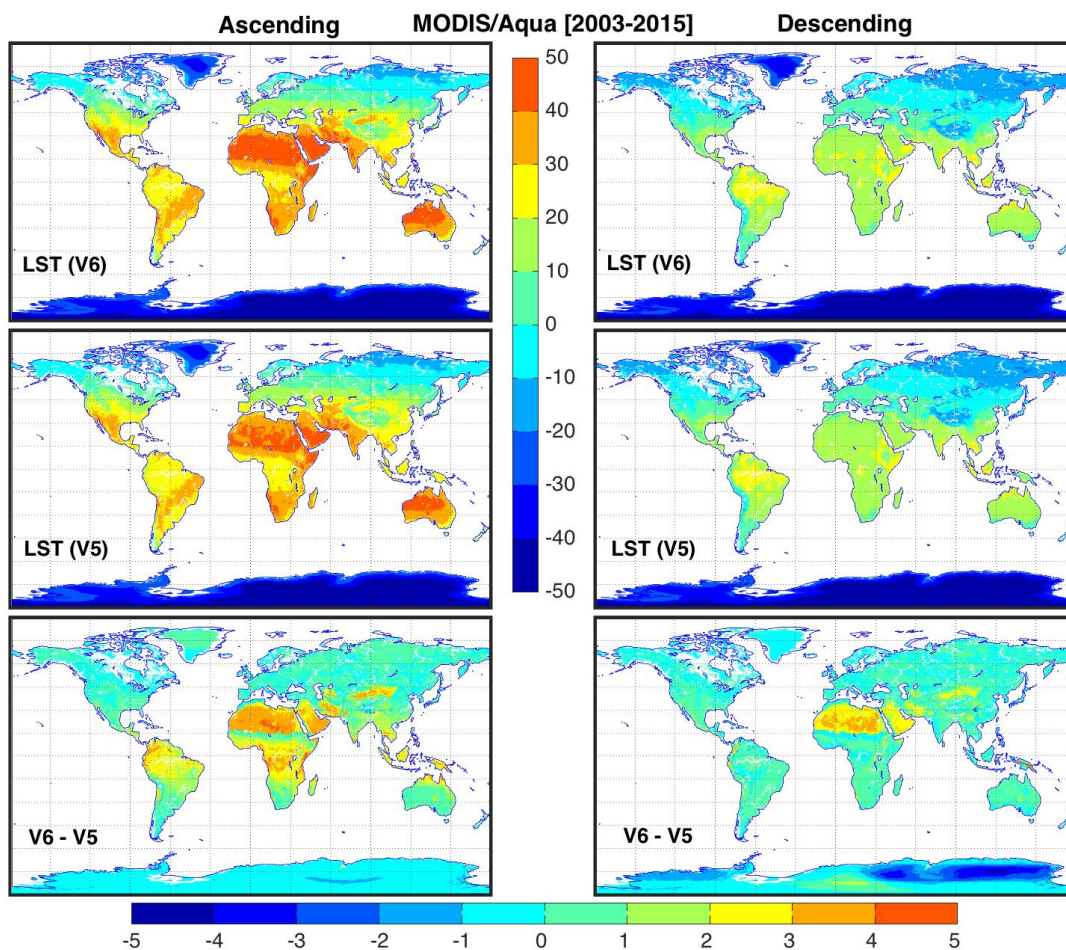


Figure 1 Spatial distributions of mean global land surface temperatures (°C) from MODIS/Aqua Version 6 and Version 5 products for day (ascending) and night (descending) overpasses, and their differences averaged for the period of January 2003 to December 2015.

Since MODIS V6 LST shows a noticeable difference from its predecessor V5 (primarily over arid regions), it appears reasonable to characterize the impact of changes in LST product versions over LSE estimates. Figure 2 shows the mean monthly global LST from MODIS V6 and V5 products and their difference for the month of January 2014. The corresponding AMSR2-derived LSE at 6.925 and 89 GHz for

horizontal polarization are also shown. Although the spatial patterns of LSE estimates are essentially similar with the use of both the versions of LST product, a considerable difference in magnitude is observed at both frequency channels over the arid regions associated with the changes in the corresponding LST product. Similarly, a notable difference in LST and LSE estimates can be seen over the Southern Polar regions. In an earlier sensitivity analysis, it was reported that a 5K difference in LST would result in an LSE retrieval differences of about 0.025, which is in good agreement with the present analysis. It is also to be noted that similar results were found for other periods. Hence, the MODIS V6 LST product is used to estimate LSE from AMSR-E and AMSR2 observations.

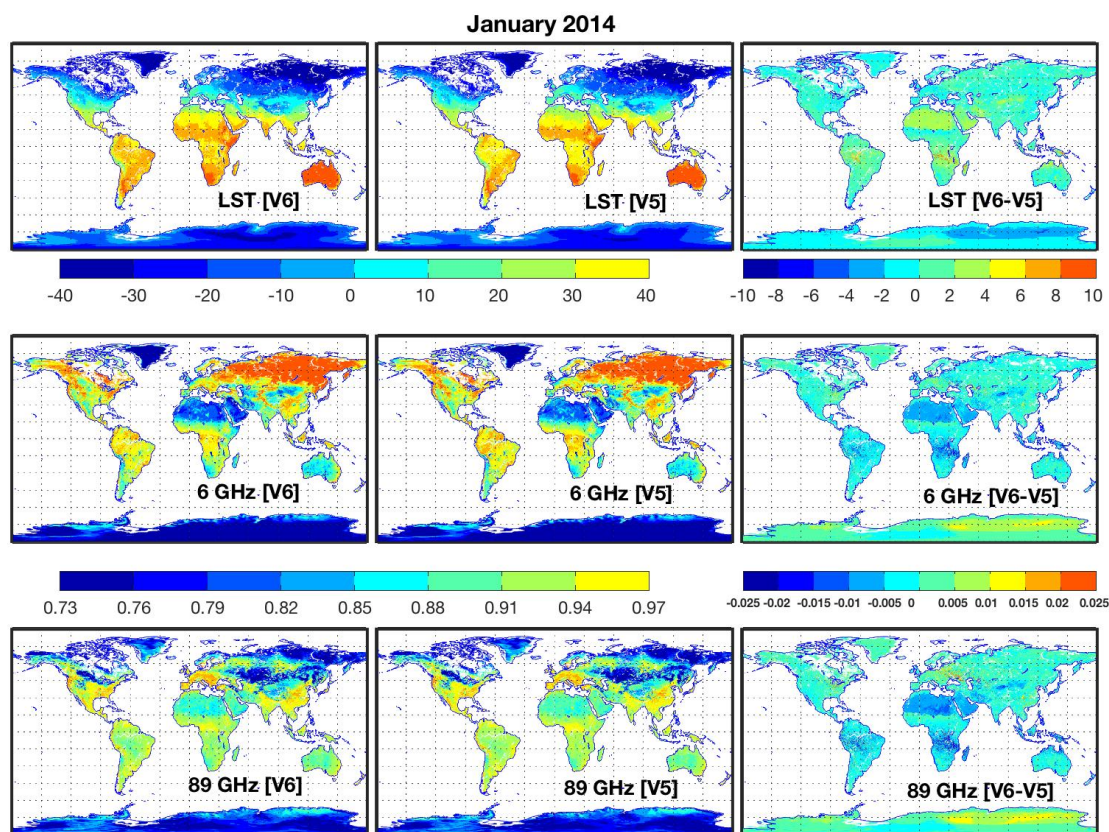


Figure 2 Mean monthly global land surface temperatures ($^{\circ}\text{C}$) from MODIS/Aqua Version 6 and Version 5 products and their differences for January 2014. The corresponding AMSR2 global land surface emissivities at 6.925 GHz and 89 GHz and their differences are also shown for horizontal polarization.

The consistency of LSE estimated by both sensors is examined for different land cover types. The comparison of global mean LSE features from the combined use of AMSR-E and AMSR2 against an independent product – Tool to Estimate Land-Surface Emissivities at Microwave frequencies version 2 (TELSEM2) showed pattern correlations of the order 0.92 at all the frequencies. Figure 3(a) shows the probability distribution functions (PDF) of LSE differences between TELSEM2 and the combined AMSR-E and AMSR2 estimates for the month of January. Both LSE estimates are in good agreement at lower frequency channels, but there is a notable difference between these two estimates at higher frequency channels. This difference might be due to water vapor and/or cloud contaminations primarily around the tropics. The corresponding mean differences in LSE between these two estimates for four different land

cover types are presented in Figure 3(b). The overestimation of LSE by the present estimates as compared to TELSEM2 linearly decreases with decrease in vegetation coverage, and notable underestimates over the desert regions. It should also be noted that there are considerable differences in sensor characteristics like incidence angle, altitude, observation time, etc. between SSM/I and AMSR-E/AMSR2.

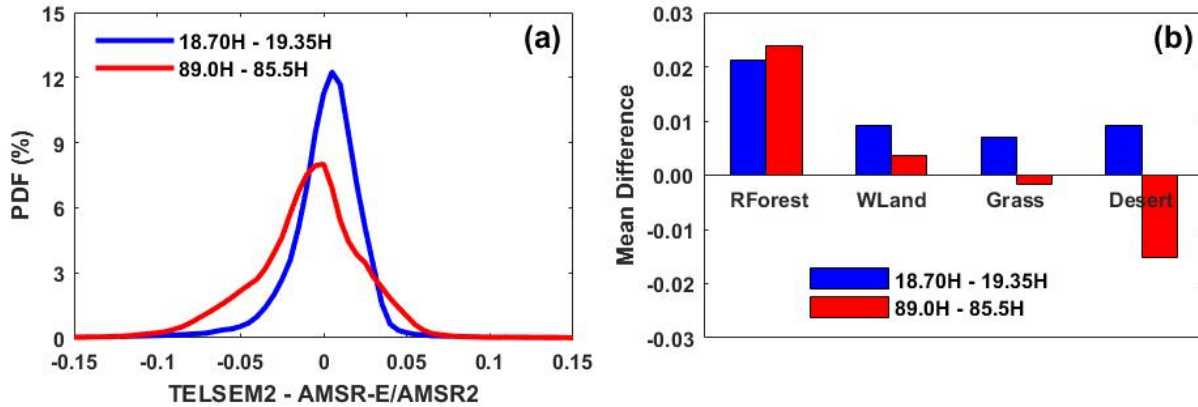


Figure 3 (a) Differences in PDF of mean land surface emissivity climatologies from TELSEM2 and combined AMSR-E/AMSR2 estimates at horizontal polarization for the month of January, and Figure 7(b) the corresponding mean difference for four distinct land cover types viz. evergreen rainforest, deciduous woodland, grassland and desert regions.

3. Assessment of Differences between Near-Surface Air and Soil Temperatures

Near-surface air temperature and the underlying soil temperature are among the key components of the Earth's surface energy budget, and they are important variables for the comprehensive assessment of global climate change. Better understanding of the difference in magnitude between these two variables over high-latitude regions is also crucial for accurate detections of freeze and thaw (FT) states. However, these differences are not usually considered and included in current remote sensing-based FT detection algorithms. The difference between near-surface air temperature at the 2-meter height and soil temperature at the 5-centimeter depth was assessed using ground-based observations that span a three-year period from 2013 to 2015. Results showed noticeable differences between air and soil temperatures over temporal scales that range from diurnal to seasonal.

Figure 4 shows daily air and soil temperatures and their differences during both day and nighttime for the three-year period for a SNOTEL station located at Colorado. Higher temperatures during the summer and lower temperatures during the winter for both air and soil correlate well with snowfall amounts. However, notable differences between both temperatures can be seen. These differences are larger during daytime than nighttime. Air temperatures show larger day-to-day variability due to insolation and weather conditions, while soil temperatures essentially vary rather slowly. Soil properties also change at slower rates due to the indirect effect of local weather conditions. The differences between these two temperatures also vary with the seasonal snow cover. The snow cover works as an effective thermal insulator due to low thermal conductivity; however, the overall impact of snow cover on the ground thermal regime depends on the duration, accumulation and melting processes of the seasonal snow cover. Hence, the variations in near-surface air temperature alone could not explain the soil temperature variations. Additionally, the presence and absence of snow cover strongly impact the surface

net radiation flux and thereby have critical climate implications. These results indicate that the upper layer soil temperature may be a more stable and effective parameter to use in FT studies than the near-surface air temperature.

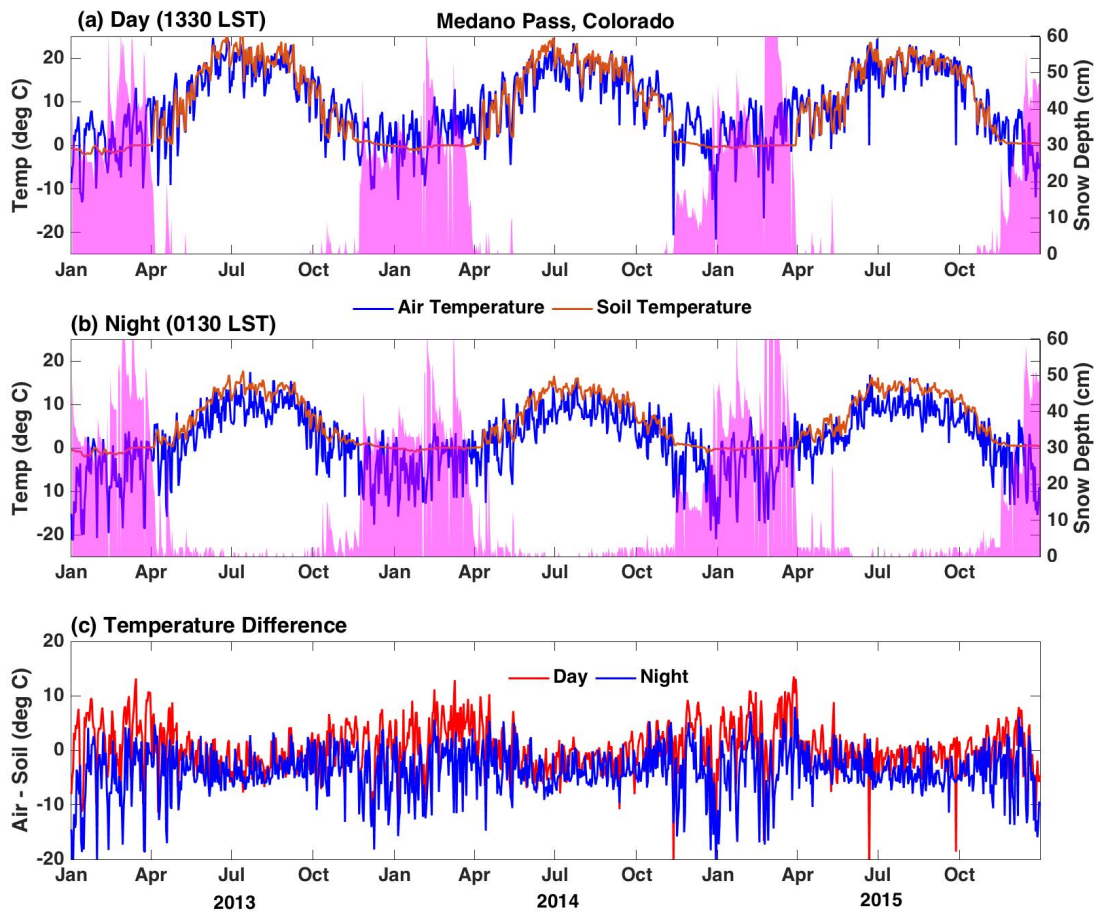


Figure 4 Time-series of daily (a) daytime and (b) nighttime near surface air temperature and soil temperature, and (c) their differences over a SNOTEL station for a three-year period (2013-2015). The shaded area in Fig. 3(a-b) represents the snow depth.

A substantial portion of the global land area exhibits seasonal FT cycles, and the transitions between freeze and thaw states depend on the magnitude and the direction of the heat energy flux and on the corresponding change in seasonal and diurnal temperatures. There are a substantial number of days observed for each station in which soil temperatures show freezing, but air temperatures show thawing, and vice-versa. Figure 5 presents the frequency of occurrence of such events during day and nighttime separately. In general, air temperature could not detect soil freezing during about 5% of daytime and more than 11% of nighttime. Similarly, air temperature could not detect soil thawing during about 7% of daytime and about 13% of nighttime. Hence, the use of air temperature for soil FT detection might lead to larger uncertainty.

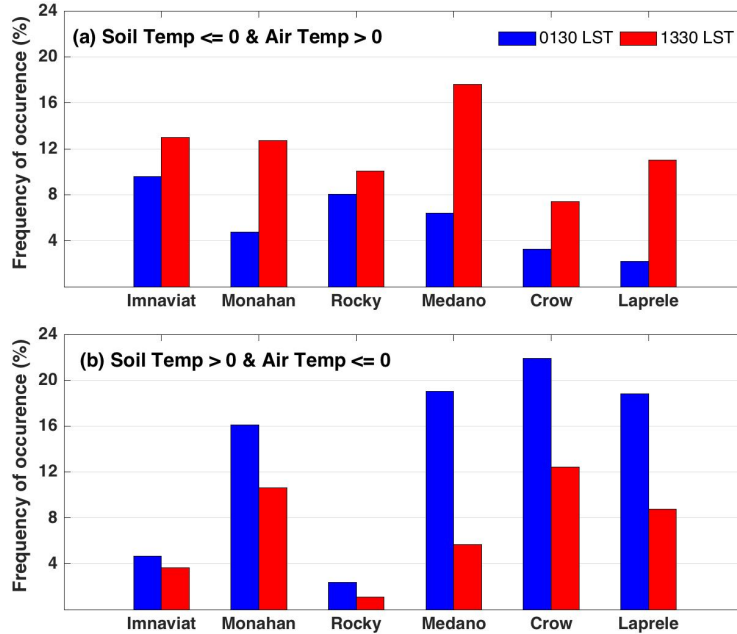


Figure 5 Difference between air temperature and soil temperature over six SNOTEL stations under two distinct cases corresponding to soil freeze and thaw states.

4. Development of an Emissivity-based Algorithm for FT Detection

Monitoring FT transitions in high latitude regions are critical to enhancing our knowledge about the prediction of biogeochemical transitions, carbon dynamics, climate change, and impacts on boreal-arctic ecosystems. Since LSE depends primarily on the surface characteristics, it would contain valuable information about the surface, especially regarding freeze and thaw states. The surface characteristics in terms of microwave emission changes whenever water undergoes phase changes at constant temperature.

we used instantaneous cloud-free land emissivity estimates from the Advanced Microwave Scanning Radiometer – 2 (AMSR2) onboard the GCOM-W1 satellite at 0.25° equal-area grids for the period of August 2012 to December 2015. In order to develop the FT detection algorithm, we used three-years (August 2012 – July 2015) of the AMSR2 land emissivity data, whereas land emissivity estimates for January 2015 to December 2015 were used for the assessment of the proposed algorithm. This land emissivity product was developed using the AMSR2 instantaneous brightness temperatures and near-simultaneous ancillary data sets such as skin temperatures from the Moderate Resolution Imaging Spectroradiometer (MODIS) and profiles of air temperature and humidity from the Atmospheric Infrared Sounder (AIRS) onboard the Aqua satellite. As brightness temperatures are affected by the atmospheric water vapor and aerosols, we used data from MODIS and AIRS instruments as ancillary to mitigate the atmospheric effects in order to compute the land surface emissivity. Moreover, the pronounced inconsistencies between the diurnal cycles of infrared-based skin temperature and PMW brightness temperatures (primarily over the arid regions) were also mitigated using a suitable statistical technique (Prakash et al., 2016a; Norouzi et al., 2015). In this technique, instantaneous MODIS skin temperatures were modified, especially over the arid regions, based on the mean skin temperature of the corresponding

month, and then land emissivity was computed for each frequency channel of the AMSR2 at horizontal and vertical polarizations separately.

We used in situ observations of soil temperature at 5 cm from 61 ground stations of the Snow Telemetry (SNOTEL) and Soil Climate Analysis Network (SCAN) available through the Natural Resources Conservation Service and National Water Climate Center (<http://www.wcc.nrcs.usda.gov/>). We used these station data sets for the development and evaluation of the FT detection algorithm. We compare our emissivity estimates with these reference ground observations to define the threshold between freeze and thaw states. Additionally, we used temperature data from the United States Climate Reference Network (USCRN; Diamond et al., 2013) and the MODIS/Aqua cloud-free land surface temperature version 5 data (MYD11C1; Wan, 2008) in this study.

Since the overpass times of the AMSR2 are 0130 LST (nighttime) and 1330 LST (daytime), we linearly interpolated in situ soil temperatures (at 5 cm) at 0100 local standard time (LST) and 0200 LST to obtain corresponding soil temperature at 0130 LST and observations at 1300 LST and 1400 LST were used to get corresponding observations at 1330 LST. Three years (August 2012 – July 2015) of AMSR2 land emissivity (the difference between emissivities of 6 GHz and 89 GHz at horizontal polarization) and 51 in situ soil temperatures were used to develop the FT detection thresholds. The choice of using the difference between AMSR2 land emissivities at 6 GHz and 89 GHz (the lowest and highest frequencies of the AMSR2) at horizontal polarization for FT detection is due to its better correspondence with upper layer soil temperatures and soil properties (Prakash et al., 2016a). We used ten distinct vegetation types (e.g., Tropical/sub-tropical evergreen broad-leaved forest, Deciduous forest, Evergreen broad-leaved and needle-leaved forest, Deciduous woodland, Sclerophyllous woodland and forest, Wooded and non-wooded grassland, Tundra and mossy bog, Boreal and xeromorphic shrubland, Non-vegetated desert, and Ice), as defined by Prigent et al. (1998) from 32 different land cover types.

Figure 6(a) shows three-year (August 2012 – July 2015) time-series of daily nighttime in-situ soil temperature at 5 cm and corresponding AMSR2 land emissivity difference between 6 and 89 GHz at horizontal polarization for a SNOTEL site over Alaska located at 65.49°N and 145.41°W. Positive (negative) soil temperature corresponds to the thaw (freeze) state and is associated with smaller (larger) magnitude of AMSR2 emissivity difference. The variables show a negative linear correlation coefficient of 0.75 with each other for the study period. Day-to-day variations in soil temperature and emissivity difference also show the transitions between freeze and thaw states qualitatively. The box plots of soil temperature and land emissivity difference for each month are shown in Figures 6(b) and 6(c). These box plots are based on the three-year daily average of nighttime (e.g., at 0130 LST) data sets, and they show the distributions of both variables. During the summer, soil temperatures are warmer and the magnitudes of corresponding emissivity difference are smaller. In general, the emissivity difference shows wider range of magnitude than soil temperature during the FT transitions period. Similar results were also found for the other SNOTEL stations. Generally, both variables are in opposite phase, and they clearly show a relationship with each other. The results convincingly show that the AMSR2 land emissivity difference of 6 GHz and 89 GHz at horizontal polarization presents significant sensitivity to soil freezing and thawing.

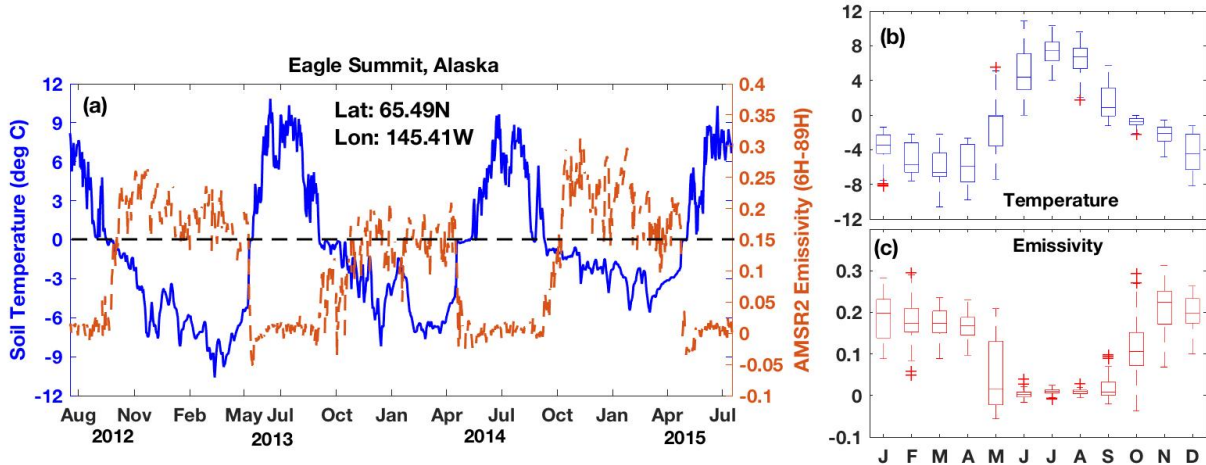


Figure 6 (a) Time-series of averaged daily at nighttime SNOTEL soil temperature at 5 cm and corresponding AMSR2-based land emissivity difference (6H-89H) for the period of August 2012 to July 2015. Box plots of the (b) soil temperature and (c) land emissivity difference for each month are also shown.

The collocated AMSR2 emissivity difference and in situ soil temperatures are binned for seven different vegetation classes for a three-year period to determine the FT thresholds. Figure 7 shows the scatter plots of binned emissivity difference and soil temperature for two vegetation classes of deciduous forest and grassland. Distinct behavior of land emissivity against upper layer soil temperature can clearly be seen for freeze and thaw states. However, the magnitude of the emissivity difference is distinct for both land cover types. The AMSR2 land emissivity difference thresholds for FT detection corresponding to 0°C soil temperature at 5 cm are estimated as 0.0261 for deciduous forest and 0.0426 for grassland. This method is repeated for the another five land cover types to obtain the corresponding thresholds. The sensitivity of different vegetation cover types to land emissivity estimates was also illustrated by Shahroudi and Rossow (2014) for snowpack detection.

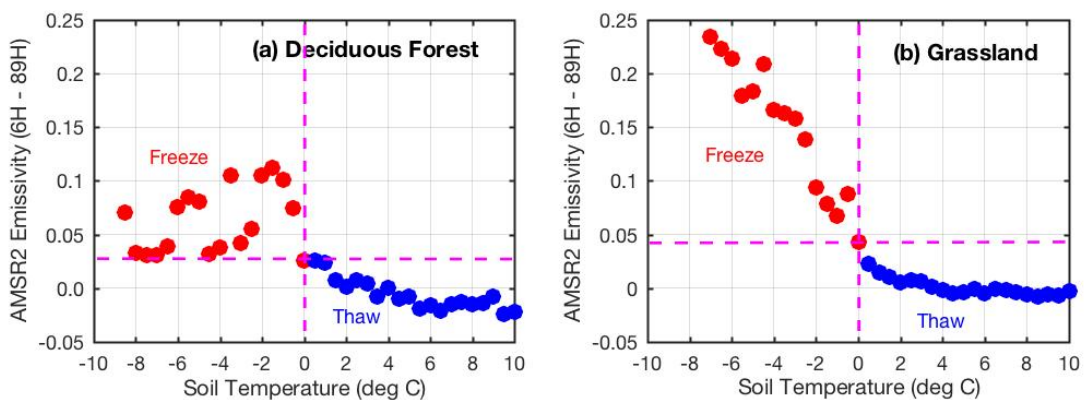


Figure 7 Scatter plots between binned AMSR2 land surface emissivity and in situ soil temperatures for (a) deciduous forest and (b) grassland areas. The binning interval is considered as 0.5°C of soil temperature in this study.

A novel threshold-based approach specific to different land cover types was developed for daily FT detection from the use of three years of AMSR2 emissivity estimates. Ground-based soil temperature observations are used as reference to develop threshold values for FT states. Figure 8 shows the spatial distributions of FT states as determined from the AMSR2 emissivity-based thresholds, for four distinct days of 2015. These FT estimates are obtained by comparing emissivity difference values and FT threshold values based on land cover type at each pixel. January is the northern hemisphere winter month when soil freezing is at its peak. April and October are transition periods, and July is the northern hemisphere summer period when soil thawing dominates. As expected, larger frozen soil area is observed during January 15th, and it starts to decrease on April 15th. During July 15th, the soil is thawed almost everywhere in the study area, and during October 15th freezing begins once again. These spatial maps are able to qualitatively depict well-known features of the soil state. Preliminary evaluation of the proposed approach with independent ground observations for the year 2015 shows that the use of land emissivity estimates for high-latitude FT detection is promising. This algorithm is being extended for the longer period of LSE estimates from AMSR-E and AMSR2 sensors in order to develop a long-term consistent global FT dataset for various applications.

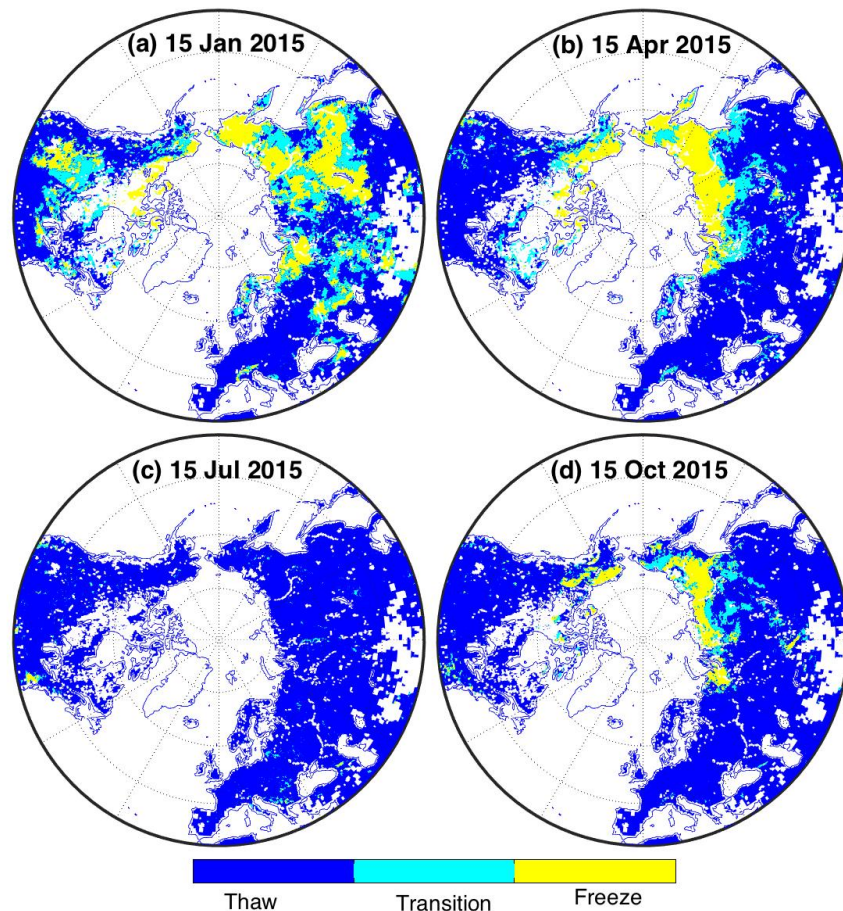


Figure 8 Daily freeze and thaw detection using AMSR2 land emissivity estimates for (a) January 15th, (b) April 15th, (c) July 15th and (d) October 15th, 2015.

These spatial maps are able to qualitatively depict well-known features of the soil state. However, quantitative evaluations are essential to assessing the potential of the present approach. For this purpose, a preliminary evaluation is performed for 2015 using 10 stations over Alaska, a region showing considerable FT characteristics (e.g., freeze-thaw transitions) over a year. The evaluation is performed at daily timescales for 2968 samples. The present approach shows a POD of 0.77, FAR of 0.07, MR of 0.23 and CSI of 0.73 (Table 1). It means that the present approach detects FT states with considerable accuracy. The evaluation is also performed for each station separately, but the results are not similar for each station. It is possibly due to differences in topography and vegetation. However, the categorical statistics showed differences with land cover types in FT detection. The uncertainty in FT detection is considerably larger for the deciduous woodland, the sclerophyllous woodland and forest than for other land cover types. Nevertheless, a comprehensive evaluation over the entire domain is required and is being planned for a longer period of time to test the robustness of this approach. This study is a first attempt to demonstrate the potential of PMW land emissivity in high-latitude FT detection with reasonable accuracy. The approach developed here can be used with multi-satellite PMW land emissivity estimates for the global FT detection, and it can also be used to adequately study soil state dynamics for various land surface applications.

Table 1 The 2×2 contingency table and categorical metrics used for the evaluation of the present algorithm at daily scale over Alaska

Estimated		Observed	
		Freeze	Thaw
	Freeze	a	b
Thaw	c	d	
Probability of Detection		POD = $a/(a+c)$	0.77
False Alarm Ratio		FAR = $b/(a+b)$	0.07
Missing Rate		MR = $c/(a+c)$	0.23
Critical Success Index		CSI = $a/(a+b+c)$	0.73

References:

Diamond, H. J., T. R. Karl, M. A. Palecki, C. B. Baker, J. E. Bell, R. D. Leeper, D. R. Easterling, J. H. Lawrimore, T. P. Meyers, M. R. Helfert, G. Goodge, and P. W. Thorne, 2013: U.S. Climate Reference Network after one decade of operations: status and assessment, *Bulletin of the American Meteorological Society*, 94, 489-498, doi:10.1175/BAMS-D-12-00170.1

Kawanishi, T., T. Sezai, Y. Ito, K. Imaoka, T. Takeshima, Y. Ishido, A. Shibata, M. Miura, H. Inahata, and R. W. Spencer, 2003: The Advanced Microwave Scanning Radiometer for the Earth Observing System (AMSR-E), NASA's contribution to the EOS for global energy and water cycle studies, *IEEE Trans. Geosci. Remote Sens.*, 41, 184-194, doi:10.1109/TGRS.2002.808331.

Norouzi, H., M. Temimi, W. B. Rossow, C. Pearl, M. Azarderakhsh, and R. Khanbilvardi, 2011: The sensitivity of land emissivity estimates from AMSR-E at C and X bands to surface properties, *Hydrol. Earth Syst. Sci.*, 15, 3577-3589, doi:10.5194/hess-15-3577-2011.

Norouzi, H., W. Rossow, M. Temimi, C. Prigent, M. Azarderakhsh, S. Boukabara, and R. Khanbilvardi, 2012: Using microwave brightness temperature diurnal cycle to improve emissivity retrievals over land, *Remote Sens. Environ.*, 123, 470-482, doi:10.1016/j.rse.2012.04.015.

Norouzi, H., M. Temimi, C. Prigent, J. Turk, R. Khanbilvardi, Y. Tian, F. A. Furuzawa, and H. Masunaga, 2015a: Assessment of the consistency among global microwave land surface emissivity products, *Atmos. Meas. Tech.*, 8, 1197-1205, doi:10.5194/amt-8-1197-2015.

Norouzi, H., M. Temimi, A. AghaKouchak, M. Azarderakhsh, R. Khanbilvardi, G. Shields, and K. Tesfagiorgis, 2015b: Inferring land surface parameters from the diurnal variability of microwave and infrared temperatures, *Phys. Chem. Earth*, 83-84, 28-35, doi:10.1016/j.pce.2015.01.007.

Okuyama, A., and K. Imaoka, 2015: Intercalibration of Advanced Microwave Scanning Radiometer-2 (AMSR2) brightness temperature, *IEEE Trans. Geosci. Remote Sens.*, 53, 4568-4577, doi:10.1109/TGRS.2015.2402204.

Prakash, S., H. Norouzi, M. Azarderakhsh, R. Blake, and R. Khanbilvardi, 2017: Potential of satellite-based land emissivity estimates for the detection of high-latitude freeze and thaw states, *Geophys. Res. Lett.*, 44, 2336-2342, doi:10.1002/2017GL072560.

Prakash, S., H. Norouzi, M. Azarderakhsh, R. Blake, and K. Tesfagiorgis, 2016: Global land surface emissivity estimation from AMSR2 observations, *IEEE Geosci. Remote Sens. Lett.*, 13, 1270-1274, doi:10.1109/LGRS.2016.2581140.

Prigent, C., W. B. Rossow, and E. Matthews, 1998: Global maps of microwave land emissivities: Potential for land surface characterization, *Radio Sci.*, 33, 745-751, doi:10.1029/97RS02460.

Prigent, C., F. Aires, and W. B. Rossow, 2006: Land surface microwave emissivities over the globe for a decade, *Bull. Amer. Meteorol. Soc.*, 87, 1573-1584, doi:10.1175/BAMS-87-11-1573.

Shahroudi, N., and W. Rossow, 2014: Using land surface microwave emissivities to isolate the signature of snow on different surface types, *Remote Sens. Environ.*, 152, 638-653, doi:10.1016/j.rse.2014.07.008.

Shati, F., S. Prakash, H. Norouzi, and R. Blake, 2018: Assessment of differences between near-surface air and soil temperatures for reliable detection of high-latitude freeze and thaw states, *Cold Reg. Sci. Technol.*, 145, 86-92, doi:10.1016/j.coldregions.2017.10.007.

Susskind, J., J. M. Blaisdell, and L. Iredell, 2014: Improved methodology for surface and atmospheric soundings, error estimates, and quality control procedures: the atmospheric infrared sounder science team version-6 retrieval algorithm, *J. Appl. Remote Sens.*, 8, 084994, doi:10.1117/1.JRS.8.084994.

Wan, Z., 2008: New refinements and validation of the MODIS land-surface temperature/emissivity products, *Remote Sensing of Environment*, 112, 59-74, doi:10.1016/j.rse.2006.06.026.

Wang, D., C. Prigent, L. Kilic, S. Fox, C. Harlow, C. Jimenez, F. Aires, C. Grassotti, and F. Karbou, 2017: Surface emissivity at microwaves to millimeter waves over Polar regions: Parameterization and evaluation with aircraft experiments, *J. Atmos. Oceanic Technol.*, 34, 1039-1059, doi:10.1175/JTECH-D-16-0188.1.